Biol. Cybern. 73, 509–518 (1995)

Biological Cybernetics



# Open-loop simulations of the primate saccadic system using burst cell discharge from the superior colliculus

S. Das [1,2], N. J. Gandhi [1,3], E. L. Keller [1,2]

[1] Smith-Kettlewell Eye Research Institute, 2232 Webster Street, San Francisco, CA 94115, USA
[2] Department of Electrical Engineering and Computer Sciences, University of California, Berkeley, CA 94720, USA
[3] Graduate Group in Bioengineering, University of California, San Francisco, CA 94143, USA

Received: 25 October 1994/Accepted in revised form: 20 June 1995

**Abstract.** Saccade-related burst neurons (SRBNs) in the monkey superior colliculus (SC) have been hypothesized to provide the brainstem saccadic burst generator with the dynamic error signal and the movement initiating trigger signal. To test this claim, we performed two sets of open-loop simulations on a burst generator model with the local feedback disconnected using experimentally obtained SRBN activity as both the driving and trigger signal inputs to the model. First, using neural data obtained from cells located near the middle of the rostral to caudal extent of the SC, the internal parameters of the model were optimized by means of a stochastic hill-climbing algorithm to produce an intermediate-sized saccade. The parameter values obtained from the optimization were then fixed and additional simulations were done using the experimental data from rostral collicular neurons (small saccades) and from more caudal neurons (large saccades); the model generated realistic saccades, matching both position and velocity profiles of real saccades to the centers of the movement fields of all these cells. Second, the model was driven by SRBN activity affiliated with interrupted saccades, the resumed eye movements observed following electrical stimulation of the omnipause region. Once again, the model produced eye movements that closely resembled the interrupted saccades produced by such simulations, but minor readjustment of parameters reflecting the weight of the projection of the trigger signal was required. Our study demonstrates that a model of the burst generator produces reasonably realistic saccades when driven with actual samples of SRBN discharges.

## 1 Introduction

The oculomotor system of primates is capable of exhibiting a rich variety of movements. Of these, saccades, quick changes of the eye's orientation from one position in the visual field to another, are perhaps the most widely studied. An extensive database on the behavior of the neurons involved in generating saccades exists. Nevertheless, with the exception of the machine-like behavior of the oculomotor neurons, the complexiy of other premotor neurons' discharge in relationship to saccades has prevented a comprehensive explanation of the neural operation of the system. Therefore, much of our knowledge of how the brain controls saccadic eye movements has stemmed from models and simulations of the oculomotor system.

An important contribution to modelling the saccadic oculomotor system in primates was made by Van Gisbergen et al. (1981) in their seminal paper. This model is based on the underlying assumption that the medium lead burst neurons (MLBNs) in the paramedian pontine reticular formation [see Keller (1981), Fuchs et al. (1985) or Moschovakis and Highstein (1994) for reviews on the types and nomenclature of neurons recorded in the reticular formation and their relationships to saccades] respond nonlinearly to a dynamic motor error signal, the instantaneous difference between the desired final eye position and the brain's estimate of current eye position. The MLBNs produce an efferent eye velocity command and project to the motoneurons (MNs) as well as to a network of tonic cells that function as a neural integrator (NI) to convert the eye velocity signal to an eye position command. These two signals together produce the pulse-step input signal recorded in MNs that in turn drives the orbital plant to yield saccadic eye movements. The output of the NI network codes an efferent copy of the instantaneous eye position and is also the feedback command to be subtracted from the desired final eye position to give the motor error. The model assumes that the feedback loop is closed locally in the brainstem and has been called the local feedback model. A saccade is initiated by a short 'trigger signal' whose origin is not specified in the model. Omnipause neurons (OPNs), which are known to inhibit the MLBNs between saccades, are disabled by this trigger signal thereby allowing

*Correspondence to:* E. L. Keller

the MLBNs to discharge. The OPNs are then held off for the duration of the saccade by a 'latch' mechanism from inhibitory MLBNs.

In another model very similar to the previous one, Jürgens et al. (1981) utilized a resettable integrator in the feedback pathway to generate a signal proportional to the instantaneous change in eye position. In their model the input thus becomes the *desired eye displacement*. For the purpose of modelling single saccades that start at the primary position, these changes are transparent, but when double saccades and/or variable initial positions are considered, the modification to *eye displacement* specifications becomes essential.

One source of the desired eye displacement signal is assumed to be the motor layers of the superior colliculus (SC), although the frontal eye fields (FEF) are probably a parallel source for this signal [see Guitton (1991) or Sparks and Hartwich-Young (1989) for reviews of SC neurophysiology]. As more fully described in these reviews, saccade metrics are coded by the spatial distribution of activity within the SC. Activity in the caudal and rostral regions is associated with large and small saccades respectively. Similarly, saccades with an upward or downward component result in SC activity medial or lateral, respectively, to the horizontal meridian.

Many additional modifications of the initial Van Gisbergen et al. (1981) model have been proposed. Most of this work is summarized in two excellent recent reviews (Guitton 1991; Moschovakis and Highstein 1994). One major variation explored is the use of an instantaneous eye velocity signal in place of an eye position signal in the local feedback loop (Scudder 1988; Lefèvre and Galiana 1992; Optican 1994). While strong arguments have been advanced for such a feedback (see, for instance, Lefèvre and Galiana 1992), another recent paper showed that a local feedback model with learning abilities could be trained to utilize either position or velocity feedback equally well (Arai et al. 1994).

The second major variation of the local feedback model explored in recent papers has been the location of the neural site of the formation of the error signal. Although this computation had originally been assumed to take place in the brainstem near the location of the burst generator, recent experiemental results have suggested that it may actually take place in the superior colliculus (Munoz et al. 1991; Waitzman et al. 1991). Although these two papers differ in the neuronal mechanism used to compute the motor error signal, both place the SC inside the local feedback loop. Models have also appeared to support one or other of the proposed mechanisms (Lefèvre and Galiana 1992; Van Opstal and Kappen 1993; Arai et al. 1994; Moschovakis 1994; Massone 1994; Optican 1994). Additional recent evidence (Keller and Edelman 1994) also supports the hypothesis that the SC is within the feedback loop.

A third development in saccadic system models has been the recent trend toward more realistic distributed processing implementations (Lefèvre and Galiana 1992; Van Opstal and Kappen 1993; Arai et al. 1994; Massone 1994; Moschovakis 1994; Optican 1994). A distributed representation becomes essential when an attempt is made to include neural structures like the SC in the model, since it is known to code information in a spatially distributed manner.

All the models which place the SC inside the local feedback loop predict that it provides at least two different types of signals to the brainstem burst generator, although the exact nature of these two classes of signals varies widely in the various models. The first type of signal can be described as a dynamic error signal. It provides the neural 'drive' to the MLBNs to create saccadic velocity. The second signal is the trigger signal used to turn off, or at least partially inhibit, OPNs to initiate the saccade.

The main objective of the present paper is to test the hypothesis that the discharge of one class of primate SC burst neuron – the saccade-related burst neurons or SRBNs [see Guitton (1991), Keller and Edelman (1994) or Sparks and Hartwich-Young (1989) for detailed descriptions of the characteristics of this type of neuron] – could provide both the signals required by a modified burst generator model. This hypothesis has been suggested on the basis of experimental results (Glimcher and Sparks 1993; Gandhi et al. 1994; Keller and Edelman 1994). In contrast to earlier models, our model uses actual spike density trains recorded from SRBNs as its inputs and these signals are used to activate the burst generator in open loop. We also attempt to capture the essential distributed nature of the SC signal processing by using data recorded from three groups of neurons located at separate SC sites. Our open-loop simulations make the implicit assumption that the feedback from the efferent sources occurs at or before the SC and that its effects are already reflected in the recorded SRBN activity. In addition, this procedure recognizes that the burst generator is shared by the upstream distributed structures of the SC and must have the same internal parameters for all saccades. Therefore, our model contains lumped elements and connections to represent the burst generator. Note that in the present paper we will consistently use the term 'burst generator' to refer to only that portion of the brainstem circuitry that generates the burst in motoneurons and includes MLBNs, OPNs, local circuit inhibitory neurons and their interconnections.

While most models produce saccades of the correct size from artificial input signals, details about the saccade trajectories are often not scrutinized carefully enough. In contrast, we perform a detailed comparison of the velocity profiles, durations and asymmetry produced by our model with real data. Because the model is driven by real SRBN discharges, temporal features of these discharges are also incorporated in it, and eliciting realistic simulated saccades would further corroborate our hypothesis concerning SRBNs supplying the burst generator inputs.

## 2 Simulation methods

### *2.1 Implementation details of the model*

In this section, we give an explicit account of the model that was used in our present simulations including the

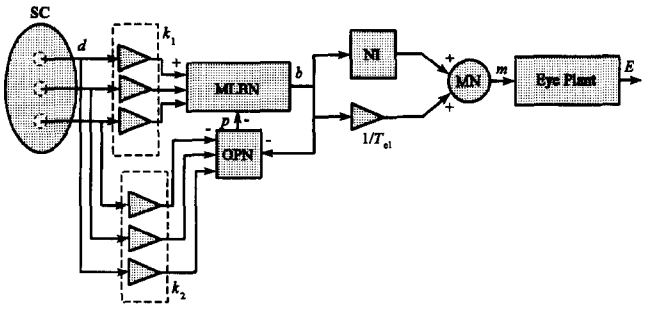


**Fig. 1.** The model. The quantity $d$ is the discharge coming from three different location in the SC, shown by three *small circles* in the latter. The gains $k_1$ and $k_2$ are represented as arrays. Only one element of each was active at a time, depending on the size of the saccade. See text for the definitions of the remaining symbols

burst generator and its inputs. The reader should refer to Fig. 1, which shows the model in simplified form, for a clarification of some of the symbols and abbreviations used here. Medium lead burst neurons (MLBNs) drive the motoneurons of the eye plant through push–pull action. Therefore in our burst generator model, the output $b(t)$ of the MLBNs actually consists of two components, $b_R(t)$ and $b_L(t)$, such that $b(t) = b_R(t) + b_L(t)$, but not explicitly shown in Fig. 1. These components are the outputs of those MLBNs that excite and inhibit the oculomotor neurons for right, horizontal saccades, respectively, and are given by,

$$b_R(t) = \begin{cases} b_m\left[1 - \exp\left(\dfrac{-(u(t) + e_0)}{b_k}\right)\right] & u(t) > -e_0 \\ 0 & u(t) \leqslant -e_0 \end{cases} \tag{1}$$

and

$$b_L(t) = \begin{cases} -b_m\left[1 - \exp\left(\dfrac{u(t) - e_0}{b_k}\right)\right] & u(t) < e_0 \\ 0 & u(t) \geqslant e_0 \end{cases} \tag{2}$$

where $b_m$ is a positive constant for the asymptotic peak discharge rate of MLBNs, $e_0$ is a small positive constant which shifts the nonlinear burst cell input/output relationship on the input axis, $b_k$ is a positive constant that determines the shape of the burst cell curve and $u(t)$ is the input to the MLBNs (Van Gisbergen et al. 1981). In our current simulations we consider only rightward saccades in which case $u(t)$ is positive, $b_R(t)$ is always positive and $b_L(t)$ is always negative. Note that this non-physiological assumption of a negative firing rate is adopted for simplification of the model only, and avoids the use of an explicit inhibitory interneuron. We placed a first-order filter between the driving signal and the MLBNs that slightly smoothed the driving signal and elicited more symmetric velocity profiles from the model. The MLBN input $u(t)$ is now given by

$$u(t) = \begin{cases} \left(1 + \tau_b \dfrac{d}{dt}\right)^{-1} k_1 d(t) & p(t) = 0 \\ 0 & p(t) > 0 \end{cases} \tag{3}$$

where the operator $d/dt$ denotes differentiation with respect to time, $\tau_b$ is the time constant of the filter and $d(t)$ is the driving signal (SRBN activity) to the MLBNs. The quantity $p(t)$ is the output of the omnipause cells (OPNs). It may be seen that (3) incorporates a switching mechanism (Lefèvre and Galiana 1992) associated with the OPNs, since the MLBNs are turned off when $p(t) > 0$. As seen below, the situation where $p(t) < 0$ does not arise.

The pauser output is

$$p(t) = \text{sgn}\left[B - k_2 d(t) - h \times |b(t - \tau_1)|\right] \tag{4}$$

The function $\text{sgn}(\cdot)$ is a sign function whose outputs are zero and unity for negative and non-negative arguments, respectively. The first term in the argument of this function in (4) is a constant bias input, the second term $k_2 d(t)$ is the trigger signal and the third term is the latch signal from inhibitory MLBNs that holds the OPNs in an inhibited state until the end of the saccade.

Finally, the input to the second-order eye plant is

$$m(t) = b(t)/T_{el} + \int_0^t b(t)\,dt \tag{5}$$

The integral term in (5) is the output of the neural integrator NI. This provides the step component of $m(t)$, while the first term in (5) provides the pulse component. The constant $T_{el}$, is the long time constant of the plant (150 ms). We used the same value (4 ms) for the short time constant of the plant as Van Gisbergen et al. (1981).

### *2.2 Preparation of the physiological signals for use as model inputs*

During a saccade a large region in the intermediate layers of the superior colliculus (SC) is active for every movement [see Sparks and Hartwich-Young (1989) or Guitton (1991) for reviews]. The center of the active region on the colliculus shifts with saccade size and direction, but only cells near the center of the active population discharge at the high frequency. Of the different types of burst cells in the intermediate layers of the monkey SC, detailed reports on the dynamic behavior of only the SRBNs are available (Waitzman et al. 1991; Keller and Edelman 1994). Because they are known to project to the region of the burst generator (Keller 1979; Moschovakis et al. 1988; Scudder et al. 1989; Istvan et al. 1994; Keller and Edelman 1993), we based our study on the SRBNs as the source of both inputs to the model.

We picked purely horizontal saccades for analysis so that the centers of the active regions on the SC lay near the representation of the horizontal meridian on the SC motor map as shown schematically in Fig. 2. We picked saccades of three different sizes: 5°, 10° and 22° (small, medium and large saccades). Additionally, we picked

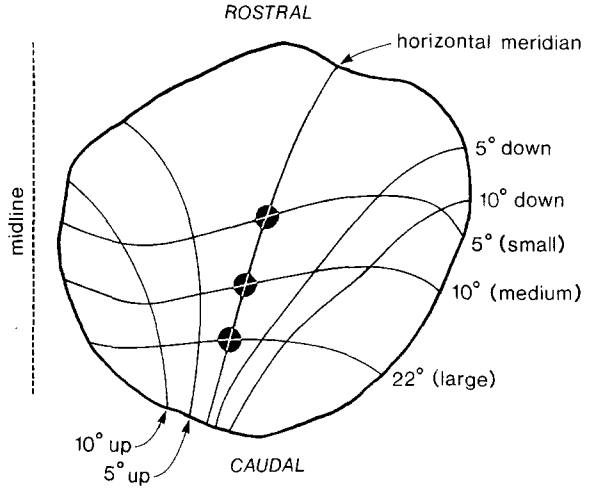


**Fig. 2.** A schematic representation of the right SC with the superimposed motor map. The grid shows the highly nonlinear mapping of the contralateral motor field. The approximate locations of the centers of activity for small (5°), medium (10°) and large (22°) saccades are indicated by *filled circles*. Modified from Cynader and Berman (1972)

resumed saccades, i.e., saccades that follow electrical stimulation of the omnipauser region for a 24° target. We provide a more complete description of such saccades at a later stage in this section. Eye movement data, as well as the neural discharge activity of SRBNs near the three regions of the SC in two monkeys (at a time resolution of 1 ms), were obtained from our previous experimental work (Keller and Edelman 1994). All raw spike trains recorded for saccades to each SRBN's movement field center were first convolved with a Gaussian smoothing function with a temporal width of 4 ms (Richmond and Optican 1987). The resulting, continuous spike density traces were then aligned with respect to saccade onset and averaged, yielding one signal per cell. Because it was not possible to determine the exact temporal lead each neuron had in influencing the saccadic system, we aligned the averaged spike density functions for the group of cells active for each size movement on their peak discharge (5 cells for the small, 6 cells for the medium, and 3 cells for the large and the interrupted saccades). Next, each sites's spike density was normalized to unity. The last step implements the usual assumption that the SRBN discharge frequency at the center of the active region on the SC has the same average peak value for any size movement (Lefèvre and Galiana 1992; Arai et al. 1994; Massone 1994).

The averaged spike density traces used in the stimulations for the small, medium and large saccades are shown in Fig. 3 (top). Our sample cells are thus intended to represent the large population of collicular cells active for each site with a single signal, while still preserving the essence of the spatially distributed nature of the SC processing by having a different, non-overlapping sample of cells active for small, medium and large saccades.

In order to test the goodness of fit of the actual monkey saccades with those produced by the simulations, we compared saccade magnitude, duration, peak velocity and velocity profile asymmetry. The last quantity was computed from the formula (Van Opstal and Van Gisbergen 1987)

$$S = D_a/D \tag{6}$$

where $S$ is the measure of symmetry (a value of 0.5 indicates a symmetric velocity profile), $D_a$ is the interval between saccade onset and peak velocity (the acceleration phase) and $D$ is the saccade duration. The epochs marking saccade beginning and end were always based on a 15°/s eye velocity criterion.

### *2.3 Simulations of normal saccades*

In our simulations, the (normalized) spike density traces were scaled by factors $k_1$ and $k_2$ before serving as the driving signal and the trigger signal, respectively, to the burst generator. As mentioned earlier, these putative control signals for the burst generator originate from different regions in the SC for saccades of different size. Hence, it seemed reasonable to allow different gains, $k_1$ and $k_2$, for each averaged spike density train. Our first goal was to adjust the parameters of the model until the simulated eye movements for medium-sized saccades (10° in amplitude) resembled those recorded in our monkeys. The model parameters that we chose to adjust were the internal parameters of bias ($B$) level to the pause cells, the delay ($\tau_1$) and the gain ($h$) associated with the inhibitory latch signal from MLBNs to pause cells, the parameters $b_m$, $e_0$ and $b_k$ of the MLBN's input/output nonlinearity; and the input scaling factors $k_1$ and $k_2$. A stochastic optimization algorithm was used to adjust both internal and input parameters simultaneously, to obtain the 'best' possible match between the model's and the monkey's performances for medium-sized saccades. A more complete description of this algorithm is discussed later. Subsequently, we manually adjusted only $k_1$ and $k_2$, separately for the small and large saccades, until a close match between the model's and the monkeys' performances was once again obtained in each case. Because the same burst generator is shared by the upstream distributed structures (e.g., the SC), it must have the same internal parameters for all saccades.

### *2.4 The optimization algorithm*

In realizing an optimal set of parameters for the local feedback model, i.e., one that produced realistic model saccades using actual spike density recordings as its input driving and trigger signals, it was assumed that the dynamics of the oculomotor plant were known. Hence the time constants of the plant were the same as those used by Van Gisbergen et al. (1981). We also chose not to vary the gains from the MLBNs and NI to the eye plant, as the correct ratio between these two gains had to be maintained to produce realistic saccades. For instance, a slightly larger value of the gain from the MLBNs produced a larger pulse component, resulting in saccadic overshoots followed by slow return movements in the opposite direction. All the other parameters, namely the bias, $B$, of the pause cells, the delay, $\tau_1$, and the gain, $h$, of

the latch mechanism, the MLBN parameters $b_m$, $e_0$ and $b_k$, and the gains $k_1$ and $k_2$ associated with the collicular projection to MLBNs and pause cells respectively, were allowed to vary during the optimization.

An overall cost function was formulated as follows:

$$\mathrm{OCF} = \alpha|PV_{\mathrm{sim}} - PV_{\mathrm{real}}|^2 + \beta|D_{\mathrm{sim}} - D_{\mathrm{real}}|^2 + \gamma|E_{\mathrm{sim}} - E_{\mathrm{real}}|^2 \quad (7)$$

The subscripts 'sim' and 'real' refer to the values obtained by performing simulations with the model and to the real values obtained from the monkeys, respectively. The first term of the OCF is minimized when the peak velocity ($PV$) of the model closely matches that of the monkeys. Similarly, the second term was chosen to bring the duration ($D$) of the model saccades as close as possible to that of the real saccades. Finally the last term was selected to minimize the difference between the model and monkey final eye displacements ($E$). The quantities $\alpha$, $\beta$ and $\gamma$ are a set of suitably chosen weights.

It was found that the OCF was highly non-linear with respect to most of the parameters that were chosen for the optimization. Treating the OCF as a junction of these parameters revealed a very complex 'terrain', with local minima. Hence the optimization was based on a stochastic hill-climbing algorithm. This approach was very similar to the simulated annealing algorithm (Kirkpatrick et al. 1983). At every iteration of the procedure, the set of parameters was perturbed, and the resulting change in the OCF was evaluated. If this was associated with a decrease in the OCF, these perturbed values were accepted as the new set of parameters. On the other hand, when the perturbation yielded an increase in the OCF the perturbed values were accepted only with a probability equal to $\exp(-c\Delta\mathrm{OCF})$ (called the acceptance probability), where $\Delta$OCF is the change in the OCF and $c$ is the control parameter of the algorithm. A non-zero acceptance probability is always chosen in highly complex optimization problems such as this, so that the algorithm does not, in a stochastic sense, get 'trapped' in a local minimum. When the control parameter is very low, the acceptance probability is close to unity. Similarly a high value of $c$ results in a very low acceptance probability.

The control parameter $c$ was initialized to a very low value. A double loop was incorporated into the algorithm. Within the inner loop a predetermined fixed number of iterations of the algorithm was allowed for a constant value of $c$. However, in each iteration of the outer loop, the control parameter was increased geometrically by a factor $\lambda$. Under these circumstances, the algorithm initially resembles a random walk over the terrain. This enables the algorithm to explore a large sample space. But since the acceptance probability is always less than unity, the algorithm is expected to approach a global minimum value of the OCF. In subsequent iterations, with an increase in the control parameter, it gradually gets transformed to a greedy algorithm. This is done so that the algorithm does not escape out of the attraction basin of this global minimum. We chose a value for $\lambda$ that was only slightly more than unity, thereby allowing a very gradual increase in $c$.

The amount of perturbation allowed for each parameter was also variable. If there was no decrease in the OCF for a very large number of iterations, the perturbations were stepped up. This helped the algorithm to move to a new (and, it was hoped, better) location. In this manner, the algorithm may be regarded as an adaptive process. If, after allowing a very large number of iterations, no further improvement in the OCF could be obtained, the algorithm was terminated. The final set of values of the model parameters and gains that were obtained from the optimization were chosen as the optimal values.

### *2.5 Simulations of interrupted saccades*

Interrupted saccades are produced by the delivery of a short train of high-frequency electrical microstimulation to the omnipause region at the onset of the movement (Keller 1977; King and Fuchs 1977). The effect of the stimulation is to stop the saccade in mid-flight. Shortly after the stimulus is turned off, the saccade resumes its course and lands close to the originally targeted position for the movement even though the visual target had been turned off before the saccade began. The perturbation in saccade dynamics, without any concomitant alteration in total saccade amplitude that occurs with interrupted saccades, provides an opportunity for critical tests for dynamic models of the saccadic system. We have used typical spike density records obtained by Keller and Edelman (1994) during interrupted saccades to test our present model further. Briefly, Keller and Edelman report that for saccades larger than 20° in amplitude, the SRBNs in the caudal colliculus became active before, and produced peak discharges just before, saccade onset. Within a few milliseconds after the onset of electrical stimulation in the omnipause region, all SRBNs were inhibited abruptly as the saccade was interrupted. Shortly after the end of the stimulation, the same group of SRBNs in the caudal colliculus that had been active at the onset of the large, targeted saccade resumed their activity just before the resumed movement, which eventually placed the eyes near the original target position. Although normal, medium-sized saccades are typically accompanied by minimal or no activity in the caudal SRBNs, resumed saccades of similar amplitude are associated with significantly stronger discharge patterns. Furthermore, recordings from SRBNs in the middle colliculus during the resumed saccade measured only minimal or no discharge for movements that would have been to the middle of their movement fields in normal circumstances. In other words, the SRBNs originally active at the onset of a large saccade were, to a first approximation, the only active SRBNs during the medium-sized resumed saccades.

We simulated the resumed saccades by aligning the averaged second burst of activity from three typical SRBNs (with movement field centers at 24°) on their peak discharge. We used this signal as the common input (driving signal and trigger) to the same open-loop model previously optimized for normal saccades. The spike density records were obtained during saccades that were

24° in total size (initial plus resumed movement). Because these SRBNs as a group were located slightly more caudally on the SC in comparison with the previously used group located at the 22° collicular locus, we extrapolated the values of $k_1$ and $k_2$ on the basis of their changes over the range from 10° and 22° to give the effective projection weights for the 24° collicular location.

## 3 Results

In Table 1 we show the final values of the internal model parameters resulting from the optimization algorithm. With the exception of the constant ($\tau_b$) for the filter which preceded the MLBNs, which was added in this study, none of the model parameters show a marked deviation from the empirically set values in Van Gisbergen et al. (1981). The values of gain parameters $k_1$ and $k_2$ obtained from our optimizations are shown in Table 2. The values for $k_1$, representing the effective weights of the collicular projections to the MLBNs from the various locations on the SC motor map, showed a non-linear increase for rostral to caudal variation in SC sites (Table 2). In contrast, the gain $k_2$ representing the projection weights from the colliculus to the OPNs was nearly equal for all three collicular regions (Table 2).

**Table 1.** Final model parameters and gains: the internal parameters of the local feedback model obtained from the optimization algorithm

| $\tau_b$ (ms) | $\tau_1$ (ms) | $B$ ($s^{-1}$) | $b_m$ ($s^{-1}$) | $e_0$ (deg) | $b_k$ | $h$ |
|---|---|---|---|---|---|---|
| 3.00 | 0.95 | 63.73 (58.00) | 755.94 | 1.82 | 12.41 | 0.12 |

The value within parentheses for the pauser bias, $B$, was for simulating interrupted saccades only

**Table 2.** Final model parameters and gains: the projection weights used for small, medium and large saccades

| | $k_1$ | $k_2$ |
|---|---|---|
| Small saccades | 7.57 | 68.25 |
| Medium saccades | 18.40 | 68.25 |
| Large saccades | 19.85 | 68.65 |
| Interrupted saccade | 20.07 | 68.71 |

Saccade size, $\Delta E$, peak velocity, $PV$, duration $D$, and symmetry, $S$, were computed for the real and the simulated movements, and the resulting values are given in Table 3. The sensitivities of $\Delta E$, $PV$ and $D$ to variation in the model parameters and gains were computed for saccades of intermediate size. The sensitivities were computed in a relative manner, as the ratio of the fractional change in the model output (e.g., $\Delta E$, $PV$ or $D$) to the fractional change in each parameter. Table 4 shows the sensitivities of the relative outputs to the model parameters and gains.

### 3.1 Simulations of normal saccades

The saccades of the three sizes produced by the model are compared with actual movements of the same sizes in Fig. 3. In this figure the averaged peak velocities of the actual movements have been aligned with respect to the averaged spike density traces such that the peak velocity occurred 15 ms after the peak SRBN discharge. This delay incorporates a similar time shift between peak collicular discharge and saccadic onset to that discussed by Waitzman et al. (1991). Figure 3 and Table 3 show that a generally good fit of saccade amplitude, peak velocity and duration was obtained with the open-loop simulations for each of the different saccade sizes. The largest percentage differences in saccade amplitude and peak velocity occurred for the large saccades (approx. 4% for amplitude and 5% for velocity). The error in

**Table 3.** Comparison between the real and model performances: the eye displacement ($\Delta E$), peak velocity ($PV$), duration ($D$), and the measure of symmetry ($S$) for the monkeys and model simulations, for saccades of each size

| | $\Delta E$ (deg/s) | $PV$ (deg/s) | $D$ (ms) | $S$ |
|---|---|---|---|---|
| *Monkey* | | | | |
| Small saccades | 5.31 | 321.26 | 25.8 | 0.496 |
| Medium saccades | 10.17 | 500.40 | 36.6 | 0.464 |
| Large saccades | 22.19 | 615.88 | 56.0 | 0.414 |
| Interrupted saccade | 11.75 | 485.83 | 54.7 | 0.371 |
| *Model* | | | | |
| Small saccades | 5.31 | 318.49 | 28.4 | 0.394 |
| Medium saccades | 10.18 | 501.18 | 34.6 | 0.329 |
| Large saccades | 21.34 | 585.94 | 53.0 | 0.287 |
| Interrupted saccade | 11.14 | 488.68 | 36.6 | 0.311 |

**Table 4.** The relative sensitivities of the simulation outputs with respect to the model parameters and gains

| | $\tau_b$ | $\tau_1$ | $B$ | $b_m$ | $e_0$ | $b_k$ | $h$ | $k_1$ | $k_2$ |
|---|---|---|---|---|---|---|---|---|---|
| $\sigma_E$ | −0.24 | 0.00 | −2.52 | 1.53 | 0.22 | −0.97 | 0.53 | 0.84 | 1.19 |
| $\sigma_{PV}$ | −0.10 | 0.00 | −0.48 | 1.00 | 0.06 | −0.51 | 0.00 | 0.49 | 0.48 |
| $\sigma_D$ | −0.12 | 0.00 | −1.74 | 0.47 | 0.12 | −0.35 | 0.38 | 0.29 | 0.58 |

The sensitivities for model simulations are for medium saccades only. They are rounded off to two decimal places. The sensitivities with respect to the parameters $b$ and $k_2$ were computed by perturbing the parameter by ± 0.5%, since larger perturbations would not allow for the initiation of the saccade. All other sensitivities were computed on the basis of ± 5% perturbation. A negative sign indicates that the change in the model's output was in a direction opposite to the corresponding change in its parameter value

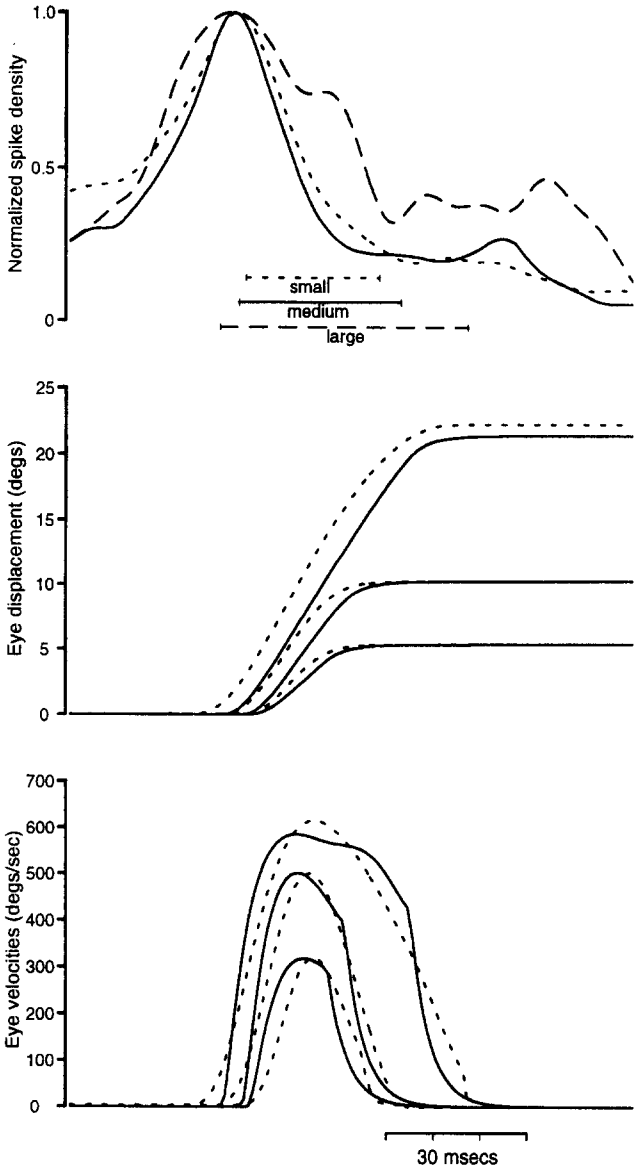


**Fig. 3.** Simulations of normal saccades. *Top*: The normalized spike density traces that were used for simulating small, medium and large saccades are shown by *dotted*, *continuous* and *dashed lines* respectively. The spike densities have been aligned so that their peaks coincide. The time intervals marking the onset and end of saccades of each size are also shown by *dotted*, *continuous* and *dashed lines*. *Middle*: The eye displacement traces for small, medium and large saccades. The simulated traces are shown in *continuous lines*. Actual eye movements of the monkeys have been shown in *dotted lines* for the sake of comparison. *Bottom*: The eye velocity traces for small, medium and large saccades. Simulated and real eye velocities are shown by *continuous* and *dotted lines* respectively

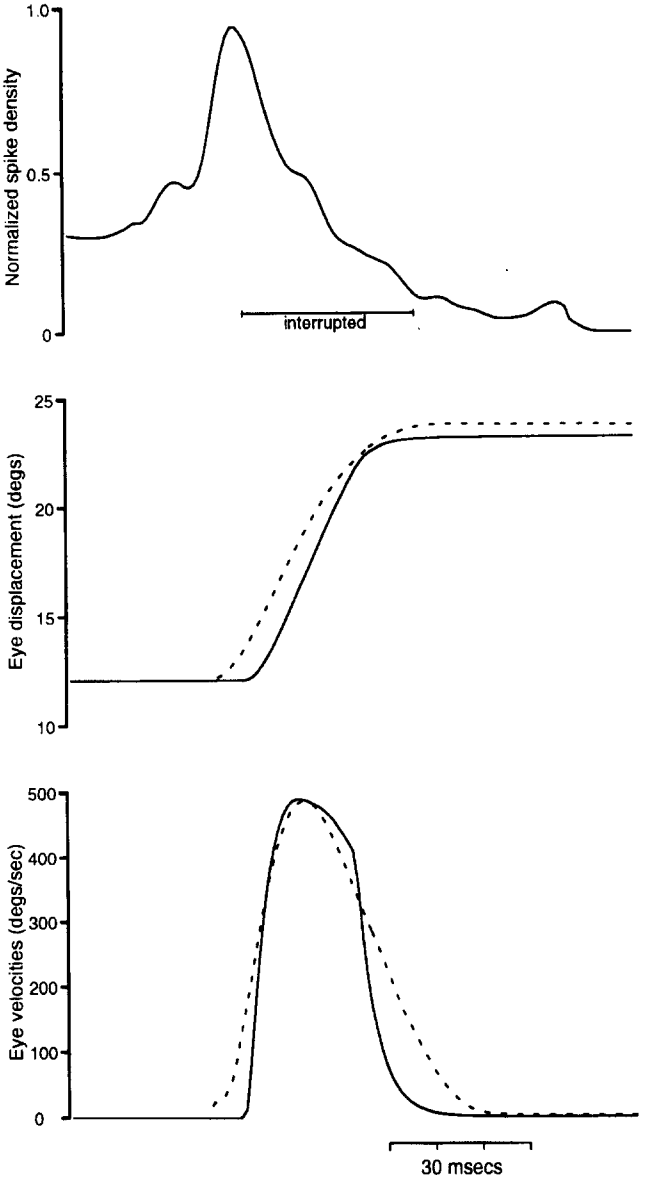


**Fig. 4.** Simulation of the resumed saccade. *Top*: The spike density train associated with the resumed saccade. Only the second peak of the discharge is shown. *Middle*: The eye displacements of the model and real saccades are shown by *continuous* and *dotted lines* respectively. *Bottom*: The eye velocities for the model and real saccades are shown by *continuous* and *dotted lines* respectively. The eye starts at a displacement of 12°, which was the average position obtained at the time of saccade interruption

duration was largest for the case of small saccades (approx. 10%). Comparison of the symmetry values indicates that the model produced considerably more asymmetric velocity profiles for all sizes of saccades, with the percentage error for large saccades being the largest (approx. 31%).

The sensitivity analysis revealed that the simulated outputs were quite sensitive to some internal parameters, particularly $B$ and $b_m$. In contrast, the sensitivities with respect to the delays were very small. Sensitivities to the gains $k_1$ and $k_2$ were also relatively high, especially for saccade amplitude.

### *3.2 Simulations of interrupted saccades*

Extrapolated values for $k_1$ and $k_2$ (Table 3) and an averaged spike density signal for the second burst of SRBN activity (Fig. 4, top) from the interrupted saccade paradigm, were used in open-loop simulations to produce realistic resumed saccades. The lower sections of Fig. 4 and Table 3 show the comparisons of the resumed saccades generated by the simulation with those of the

monkeys. The resumed saccades of the monkeys are slower than they should be on the basis of their size. Notice that the average monkey resumed saccade, which is about 12° in amplitude, exhibits a peak velocity that is actually lower than normal 10° movements and a duration that is almost as long as normal 22° saccades, i.e., they are considerably displaced from the stereotyped main sequence for saccades. The saccades created by the simulation capture some of the behavior of the monkey resumed saccades – they are only about 5% different in size and have very similar peak velocities. However, they do not have the longer durations of the monkey saccades.

The results of the resumed saccade simulations can be partly explained by careful observation of the spike density function (the second burst of SRBN activity) that accompanies resumed movements. Because our normalization of the burst signal sets the peak associated with the saccade onset to unity, the resulting peak of the second burst is less than one. As a result, the activity associated with the resumed saccade was not quite as large as that at the start of the initial saccade – a relationship that is also observed experimentally (Keller and Edelman 1994). The spike density trace in Fig. 4 (top) peaks at only 0.94 after normalization. We found that this level of activity, although larger than might be expected if the SRBN discharge were used only as a dynamic error signal, was not sufficient to turn off the pause cells to initiate the resumed saccade. Therefore we lowered the bias signal, $B$, on the pause cells to 58 for this experiment. All other parameters within the burst generator remained fixed at the values in Tables 1–3.

We also attempted to produce the resumed saccade by using the same SRBN discharge profiles but with the gains, $k_1$ and $k_2$ that were appropriate for the medium-sized saccades. In this simulation the model produced a resumed movement with $\Delta E = 9.65°$, $PV = 446.36°/s$ and $D = 35.4$ ms. Clearly, the gain values associated with the larger, 24° collicular site produced a resumed movement that more closely resembled the monkey resumed saccade. This observation supports the finding of Keller and Edelman (1994) that it is resumed activity at the original collicular site that produces the second movement.

## 4 Discussion

### *4.1 SRBNs may provide both the driving signal and the saccade initiating signal to the burst generator*

The most significant result of the present simulations of the saccadic system is the demonstration that the signal produced by one class of widely studied neuron in the superior colliculus (SC), the saccade-related burst neurons (SRBNs), may be *sufficient* to provide both the dynamic saccadic error signal and the saccade-initiating trigger signal to the brainstem burst generator. We have made the following assumptions in arriving at this demonstration of sufficiency: (1) The SRBNs are inside the feedback loop computing error, and thus their temporal discharge reflects the neural computations that compare desired eye displacement and instantaneous eye displacement during saccades. This assumption was suggested by the experimental observations on SRBNs (Waitzman et al. 1991) and is further supported by the recent results of Keller and Edelman (1994). Therefore, our simulations using actual SRBN discharge as the inputs to MLBNs and OPNs were performed in open-loop mode. (2) Because only one from the set of sample collicular neurons was considered active for each size of saccade studied, a distributed input from the colliculus was required. Furthermore, each SRBN was normalized and its effect was modulated by projection weights at the burst generator. (3) The role of the burst generator is common to all saccades and therefore was modelled using lumped elements as in Van Gisbergen et al. (1981).

An optimization algorithm was used to determine a set of parameters in the burst generator that would produce a realistic saccade for one size of movement (10°), when the appropriate SRBN activity from the middle region of the SC was used as the dual-purpose input. The internal parameters within the burst generator were then fixed, and with adjustment of only the gains ($k_1$ and $k_2$) from the other regions of the SC, the model was able to produce realistic saccades of the other two sizes (5° and 22°). Adjustment of the gains for different regions of the colliculus represents the fact that while the burst generator is common to saccades of all sizes, different neurons in the colliculus are active for saccades of different sizes, and that they may project with different weights to the burst generator, as previously suggested by Scudder (1988) and Moschovakis (1994). Results obtained with the present simulations predict that projections from the caudal colliculus (the region around the 22° locus on the motor map shown in Fig. 2) to burst cells in the brainstem burst generator should be considerably stronger than more rostral connections. The increase in strength by a factor of 2.62 (see $k_1$ in Table 2) is similar to, though somewhat lower than, those in the MSH and WOMW models of Moschovakis (1994), where connection strengths differ by factors of approximately 6.02 and 5, respectively, between similar SC locations. Similar patterns of increase in connection strengths have been predicted elsewhere in recent, fully distributed SC models (Arai et al. 1994; Massone 1994). Also, the simulations suggest, as assumed by Scudder (1988) and Moschovakis (1994), that projections from all regions of the SC to OPNs may be approximately equal ($k_2$). Both predictions concerning projection weights should have an anatomical substrate, but seem not to have been closely examined in the monkey (Büttner-Ennever and Büttner 1988). An alternate mechanism for heightening the driving signal for the caudal colliculus has been reported in a study in the cat in which it was shown that the density of collicular neurons projecting to the region of the burst generator increases in the caudal colliculus (Edwards and Henkel 1978).

We also attempted to produce realistic eye movements with our open-loop model using artificial Gaussian signals in place of SRBN discharge. The model parameters, as well as the shape of the Gaussian signal, were optimized by means of our algorithm to produce

the most realistic intermediate saccade and then $k_1$ and $k_2$ were adjusted to obtain the best possible small and large saccades. While the Gaussian input elicited realistic 5° and 10° movements, the larger 22° saccades had a peak velocity of 707.58°/s, with a duration of only 47.1 ms (not shown). The error in saccade velocity is more than 18% and in duration is about 20% (in comparison with actual monkey saccades). These errors are more than twice as big for large saccades in comparison with our simulations using actual SRBN discharge. While other models (Scudder 1988; Moschovakis 1994) have used Gaussian or pulsatile functions as inputs to the burst generators, these models were evaluated under closed-loop simulations, which are less sensitive to disturbances. Moreover, the velocity profiles that were generated by the closed-loop models were not compared with real saccades as closely as in the present simulations. Our open-loop simulations using a movement size invariant Gaussian input indicate that realistic saccades of all sizes are not generated by such an input and that the temporal discharge patterns of the SRBNs incorporate features that are manifested in the resultant eye movements. These experiments therefore lend further support to the hypothesis that SRBNs provide dynamic control signals to the downstream burst generator.

However, the SRBNs are not the only output cells of the colliculus. Istvan et al. (1994) have shown that in primates, buildup neurons (BUNs) and fixations cells (FNs) may also project to the burst generator. BUNs are located in the ventral intermediate layer of the SC and exhibit an accelerating discharge for a prolonged period that begins well before saccade onset (Munoz and Wurtz 1993a). They may also be involved in spatial coding of the driving signal to the MLBNs (Optican 1994). FCs are also located in a similar layer, but only in the most rostral pole of the SC. They show a pause in discharge during saccades and may also be involved in providing dynamic control signals to the burst generator (Munoz and Wurtz 1993b). In addition to the present classification of SC neurons, other earlier schemes have been proposed for the monkey (Sparks et al. 1976) and for the cat (Harris 1980; Straschill and Hoffmann 1970; Straschill and Schick 1977).

### *4.2 A comparison between the role assigned to the SC in previous models and the present model*

Most previous distributed models of the saccadic system have used one signal from the colliculus to control saccade dynamics and a separate signal to initiate saccades (Van Gisbergen et al. 1981; Lefèvre and Galiana 1992; Van Opstal and Kappen 1993; Optican 1994). Other models have suggested that one signal from the colliculus may provide both inputs to the burst generator (Scudder 1988; MSH and WOMW models of Moschovakis 1994). However, the Scudder and MSH models place the colliculus upstream from the formation of the local feedback loop and assume Gaussian-shaped (in time) collicular discharge profiles that are invariant for saccade size. Accumulating experimental evidence suggests instead that SRBNs in the colliculus are inside a feedback loop (Waitzman et al. 1991; Keller and Edelman 1994). The results obtained with our model which drives the burst generator with actual signals obtained from SRBNs in open loop provides additional evidence for the hypothesis that the SC is inside a feedback loop, but cannot eliminate the possibility that other downstream feedback pathways are present (Optican 1994).

### *4.3 Interrupted saccades*

Several simulations (Scudder 1988; Arai et al. 1994; Moschovakis 1994) have attempted to explain the mechanism underlying the end-point accuracy of eye position observed in the interrupted saccade paradigm. Models that place the SC outside the feedback loop (Scudder 1988; MSH model of Moschovakis 1994) assume Gaussian profiles in the collicular neurons. Neither considers any change in the standard trajectory of collicular activity during an interrupted saccade. In its published form, the WOMW model (Moschovakis 1994), which does include the SC within the feedback loop, produces collicular activity that remains constant during OPN stimulations. The SC activity assumed by all three models differs from the experimental demonstration that collicular SRBN discharge is inhibited by OPN stimulation and that it remains silenced for some time after the pauser stimulation is turned off before discharging a second burst of activity in association with the resumed saccade (Keller and Edelman 1994).

The results we obtained with our model reproduced only some of the characteristics of the resumed saccade (saccade size and slower velocity) and only for one size of movement. We also had to lower the bias signal on OPNs cells to obtain retriggering, suggesting that other collicular signals may play a role in initiating saccades. A logical candidate would be the signal from FNs in the rostral zone of the colliculus (Munoz and Wurtz 1993b), as already discussed above. Future research should also include a much wider range of sizes of resumed saccades.

### *4.4 Details on the velocity trajectory shapes*

The present modelling results are the first to show detailed comparisons between simulated and actual velocity profiles, and not just the peak velocity and duration of these movements. All the published models can produce saccades of the correct size but details about the entire velocity profiles, durations and asymmetry are often lacking. We believe that our open-loop optimization procedure has produced a good set of parameters for the burst generator portion of future models and that the sensitivity analysis (Table 4) provides useful information about the effect of burst generator parameters on saccade behavior under the constraints of our assumptions listed above. The remaining differences in our velocity profiles in comparison with actual monkey saccades include two consistent features. The simulated velocities had corners (derivative discontinuities) on their trailing edges. This was more prominent in the case of the larger saccades. The corners appear as a result of steps in rapid deceleration of the simulated eye movements, as soon as the

OPNs were turned back on. The eye velocity profiles following this anomaly were purely the step response of the second-order eye plant and its compensating lead/lag network (the parallel connection of burst cells and neural integrator to motoneurons which effectively eliminates the long time constant of the plant). The other noticeable difference was that the simulated velocity profiles always had more abrupt initial accelerations than the actual movements. We tried without success to alleviate both these differences by using a different model of the plant (Optican and Miles 1985). We believe that both discrepancies could be reduced with a more distributed model of the burst generator in which not all neurons were absolutely synchronized. This is particularly important in the case of motoneurons and OPNs in which there is some temporal jitter in the onset and offset of the saccade-related burst of activity across the pool of active cells (Keller 1981; Fuchs et al. 1985).

*Acknowledgements.* This research was supported by NIH grants EY06860 and 5T32 GM08155 and an NSF grant IBN-9511365, a Rachel C. Atkinson Fellowship to S.D. and an ARCS Foundation Fellowship to N.J.G.

## References

Arai K, Keller EL, Edelman JA (1994) Two-dimensional neural network model of the primate saccadic system. Neural Networks 7:1115–1135

Büttner-Ennever JA, Büttner U (1988) The reticular formation. In: Büttner-Ennever JA (ed) Neuroanatomy of the oculomotor system. Elsevier, Amsterdam, pp 119–176

Cynader M, Berman N (1972) Receptive-field organization of monkey superior colliculus. J Neurophysiol 35:187–201

Edwards SB, Henkel CK (1978) Superior colliculus connections with the extraocular motor nuclei in the cat. J Comp Neurol 179:451–468

Fuchs AF, Kaneko CRS, Scudder CA (1985) Brainstem control of saccadic eye movements. Annu Rev Neurosci 8:307–337

Gandhi NJ, Keller EL, Hartz KE (1994) Interpreting the role of collicular buildup neurons in saccadic eye movement control. Soc Neurosci Abstr 20:141

Glimcher PW, Sparks DL (1993) Effects of low-frequency stimulation of the superior colliculus on spontaneous and visually guided saccades. J Neurophysiol 69:953–964

Guitton D (1991) Control of saccadic eye and gaze movements by the superior colliculus and basal ganglia. In: Carpenter RHS (ed) Eye movements. CRC Press, Boca Raton, Fl, pp 244–276

Harris LR (1980) The superior colliculus and movements of the head and eye in cats. J Physiol (Lond) 300:367–391

Istvan PJ, Dorris MC, Munoz DP (1994) Functional identification of neurons in the monkey superior colliculus that project to the paramedian pontine reticular formation. Soc Neurosci Abstr 20:141

Jürgens R, Becker W, Kornhuber HH (1981) Natural and drug induced variations of velocity and duration of human saccadic eye movements: evidence for control of a neural pulse generator by local feedback. Biol Cybern 39:87–96

Keller EL (1977) Control of saccadic eye movements by midline brainstem neurons. In: Baker R, Berthoz A (eds) Control of gaze by brainstem neurons. Amsterdam, Elsevier

Keller EL (1979) Colliculo-reticular organization in the oculomotor system. Prog Brain Res 50:725–734

Keller EL (1981) Brainstem mechanisms in saccadic control. In: Fuchs AF, Becker W (eds) Progress in oculomotor research. New York, Elsevier/North-Holland

Keller EL, Edelman JA (1993) Effect of electrical stimulation in the omnipause region on cells in the superior colliculus of the monkey. Soc Neurosci Abstr 19:857

Keller EL, Edelman JA (1994) Use of the interrupted saccade paradigm to study spatial and temporal dynamics of saccadic burst cells in superior colliculus in monkey. J Neurophysiol 72: 2754–2770

King WM, Fuchs AF (1977) Neuronal activity in mesencephalon related to vertical eye movements. In: Baker R, Berthoz A (eds) Control of gaze by brainstem neurons. Amsterdam, Elsevier

Kirkpatrick S, Gelatt CD, Vecchi MP (1983) Optimization by simulated annealing. Science 20:671–680

Lefèvre P, Galiana HL (1992) Dynamic feedback to the superior colliculus in a neural network model of the gaze control system. Neural Networks 5:871–900

Massone LE (1994) A neural-network system for control of eye movements: basic mechanisms. Biol Cybern 71:293–305

Moschovakis AK (1994) Neural network simulations of the primate oculomotor system. I. The vertical saccadic burst generator. Biol Cybern 70:291–302

Moschovakis AK, Highstein SM (1994) The anatomy and physiology of primate neurons that control rapid eye movements. Annu Rev Neurosci 17:465–488

Moschovakis AK, Karabelas AB, Highstein SM (1988) Structure–function relationships in the primate superior colliculus. II. Morphological identity of presaccadic neurons. J Neurophysiol 60:263–302

Munoz DP, Wurtz RH (1993a) Interactions between fixation and saccade neurons in primate superior colliculus. Soc Neurosci Abstr 19:787

Munoz DP, Wurtz RH (1993b) Fixation cells in monkey superior colliculus. I. Characteristics of cell discharge. J Neurophysiol 70:559–575

Munoz D, Guitton D, Pelisson D (1991) Control of orienting gaze shifts by tecto-reticulo-spinal system in the head-free cat. III. Spatiotemporal characteristics of phasic motor discharges. J Neurophysiol 66:1642–1666

Optican LM (1994) Control of saccade trajectory by the superior colliculus. In: Fuchs AF, Brandt T, Büttner U, Zee DS (eds) Contemporary ocular, motor and vestibular research: a tribute to David A. Robinson. Georg Thieme, Stuttgart

Optican LM, Miles FA (1985) Visually induced adaptive changes in primate saccadic oculomotor control signals. J Neurophysiol 54:940–958

Richmond BJ, Optican LM (1987) Temporal encoding of two-dimensional patterns single units of primate inferior temporal cortex. II. Quantification of response waveform. J Neurophysiol 57:147–161

Scudder CA (1988) A new local feedback model of the saccadic burst generator. J Neurophysiol 59:1455–1475

Scudder CA, Highstein S, Karabelas T, Moschovakis A (1989) Anatomy and physiology of long-lead burst neurons. Soc Neurosci Abstr 15:238

Sparks DL, Hartwich-Young R (1989) The deep layers of the superior colliculus. Oculomotor Res 3:213–255

Sparks DL, Holland R, Guthrie BL (1976) Size and distribution of movement fields in the monkey superior colliculus. Brain Res 113:21–34

Straschill M, Hoffmann KP (1970) Activity of movement sensitive neurons of the cat's tectum opticum during spontaneous eye movements. Exp Brain Res 11:318–326

Straschill M, Schick F (1977) Discharge of superior colliculus neurons during head and eye movements of the alert cat. Exp Brain Res 27:131–141

Van Gisbergen JAM, Robinson DA, Gielen S (1981) A quantitative analysis of generation of saccadic eye movements by burst neuron. J Neurophysiol 45:417–441

Van Opstal AJ, Van Gisbergen JAM (1987) Skewness of saccadic velocity profiles: a unifying parameter for normal and slow saccades. Vision Res 27:731–745

Van Opstal AJ, Kappen H (1993) A two-dimensional ensemble coding model for spatial–temporal transformation of saccades in monkey superior colliculus. Network 4:19–38

Waitzman DA, Ma TP, Optican LM, Wurtz RH (1991) Superior colliculus mediate the dynamic characteristics of saccades. J Neurophysiol 66:1716–1737